The influence of protonation on molecular structure and physico-chemical properties of gossypol Schiff bases†

Piotr Przybylski,*[a] Krystian Pyta,[a] Justyna Czupryniak,[b] Barbara Wicher,[a] Maria Gdaniec,[a] Tadeusz Ossowski[b] and Bogumił Brzezinski[a]

Received 18th June 2010, Accepted 8th September 2010
DOI: 10.1039/c0ob00288g

Protonation of gossypol Schiff bases (**S1** and **S2**), possessing different numbers of basic N-atoms, was studied using potentiometric, spectroscopic, ESI MS and PM5 methods. Titration of **S1** and **S2** with $HClO_4$, monitored by the FT-IR and ^1H NMR, indicated that the change from the enamine-enamine into the protonated imine-imine tautomeric form occurs at different Schiff base–H^+ ratio. The FT-IR and PM5 results show that for **S1** the first protonation step occurs at Schiff base moiety whereas for **S2** it is realised at N-atom of the morpholine. The formation of N^+–H ··· O hydrogen bond between morpholine moieties within **S2** contributes to high $pK_{a(ACN)} = 22.65$.

Introduction

Gossypol (Scheme 1) is present in the seeds, leaves and roots of the cotton plants and is involved in defence mechanisms against animals and insects.[1] This important natural product exhibits a variety of biological activities, including among others antiviral, anticancer or antimalarial.[2–6] Unfortunately it is also toxic and evokes many adverse effects towards cattle, fish and human.[7–10] Its toxicity has been mainly related to the presence of aldehyde groups, although, recently it has also been suggested that the phenolic groups are equally important in this aspect.[11,12] Various derivatives of gossypol with modified aldehyde[13–15] and phenolic[16,17] groups as well as the C-4 position[18] have been synthesised in search for active compounds with lower toxicity and improved biological activity. Jiang *et al.*[12] through a simple chemical modification of optically active gossypol with chiral and achiral amines obtained derivatives of higher anticancer activity than gossypol. Recently, we have shown that conversion of gossypol into its Schiff bases and hydrazones generally improved biological properties and resulted in increased affinity toward metal cations.[19–21] In view of potential applications of these compounds in medicine and agriculture there is a need to learn more about their acid–base properties and molecular structures to help structure–activity studies. Although a vast number of gossypol derivatives have been synthesised, only a few have their crystal structures reported.[20,22–31] Moreover, in view of recent reports relating the cytotoxicity of gossypol to its phenolic nature,[12] we believe that tautomerism of gossypol and its derivatives remains an important issue as it influences the number of phenolic groups within their molecules (Scheme 1).[32–35]

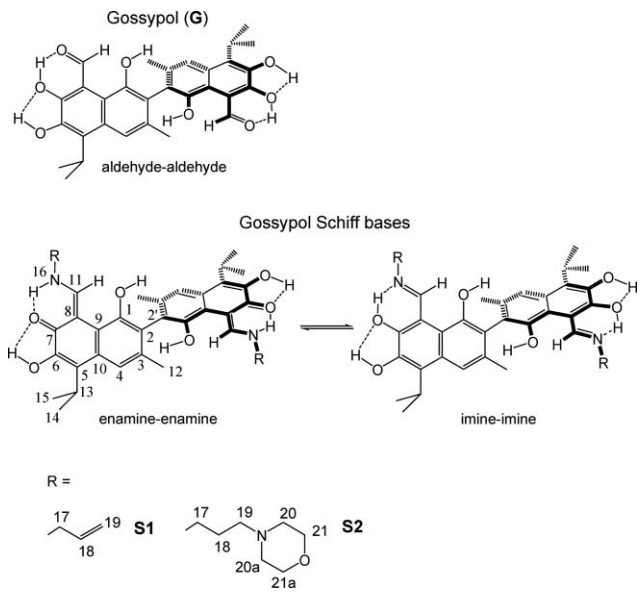

Scheme 1 Atom numbering (applied exclusively for the spectroscopic studies) together with the structure of gossypol and the possible tautomeric forms of its Schiff bases.

The number of the basicity sites within the gossypol derivatives was indicated on the basis of the potentiometric, ESI MS, FT-IR and PM5 semi-empirical studies. The molecular structures of the protonated gossypol Schiff bases with allyl amine (**S1**) and 3-morpholinopropylamine (**S2**) were investigated using FT-IR and PM5 semi-empirical methods upon the addition of various amounts of the acid. Furthermore, in this study for the first time the pK_a values of biologically active gossypol Schiff bases were determined. The crystal structure of unprotonated **S2** is reported for comparison.

Results and discussion

The structure of gossypol Schiff bases in solid and solution

The **S2** molecule in the conformation adopted in the solid state is shown in Fig. 1. In the crystal **S2** exists in the enamine-enamine tautomeric form, as evidenced by the bond lengths of the carbonyl groups in the two enaminone fragments [1.289(2) and 1.273(3) Å]

[a]*Faculty of Chemistry, Adam Mickiewicz University, 60-780, Poznań, Grunwaldzka 6, Poland*
[b]*Faculty of Chemistry, University of Gdansk, Sobieskiego 18, 80-952, Gdańsk, Poland. E-mail: piotrp@amu.edu.pl; Fax: +48 061 829 1505; Tel: +48 61 8291252*

† Electronic supplementary information (ESI) available: Spectra and additional data. CCDC reference number 763715. For ESI and crystallographic data in CIF or other electronic format see DOI: 10.1039/c0ob00288g

Table 1 ESI data of the protonated **S1** and **S2** gossypol Schiff bases, recorded at cv = 10 V in acetonitrile

Schiff base	Schiff base : $HClO_4$ stoichiometry	*m/z* signal			
		$[M + H]^+$	$[M + 2H]^{2+}$	$[M + 3H]^{3+}$	$[M + 4H]^{4+}$
S1	1 : 1	597	—	—	—
	1 : 2	—	299	—	—
S2	1 : 1	771	—	—	—
	1 : 2	—	386	—	—
	1 : 3	—	—	258	—
	1 : 4	—	—	—	194

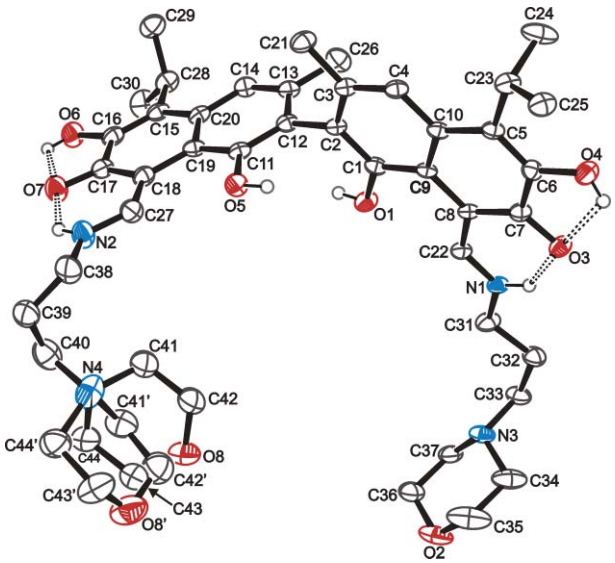

Fig. 1 The ORTEP representation of the **S2** molecule with the atom-numbering scheme as applied in the X-ray analysis. The displacement ellipsoids are shown at the 50% probability level. The H atoms bonded to C atoms are omitted for clarity.

and the location of hydrogen atoms at the bonding distance to the nitrogen atoms. These features are common for all gossypol Schiff bases reported up to now.[20,22–31] The two propyl-morpholine substituents of **S2** adopt different conformations that place centroids of the two morpholine groups at an intramolecular distance of 8.80–9.54 Å (one of the morpholine groups is disordered over two positions). There are two intermolecular O–H···O hydrogen bonds joining molecules of **S2** into two dimensional assembly and one of them involves a morpholine O atom as a hydrogen bond acceptor (for more details about the crystal structure of **S2** deposited as CCDC 763715, see Supplementary Data†).

It is well known that gossypol in its numerous crystalline forms was found exclusively as the aldehyde-aldehyde tautomer (Scheme 1).[36,37] A comparison of the FT-IR spectra of gossypol with those of the Schiff bases **S1** and **S2** in crystals is shown in Fig. 1Sa and b.† In the FT-IR spectrum of the aldehyde-aldehyde tautomer of gossypol the bands assigned to the ν(C═O) stretching vibrations of aldehyde group as well as to the ν(C═C) stretching vibrations of naphthalene rings are found at 1624 and 1573 cm^{-1}, respectively. In the FT-IR spectra of **S1** and **S2**, instead of the band of the ν(C═O) stretching vibration of the aldehyde group, another band of relatively high intensity arises at about 1628 cm^{-1}. The new band is assigned to the ν(C═O) vibrations of ketone moieties at C-7 and C-7′ positions of the naphthalene rings (Fig. 1) and its presence is an evidence of the formation of the enamine-enamine tautomeric form within the Schiff bases in the solid. This finding is in agreement with the X-ray data obtained for **S1**[25] and **S2** (Fig. 1). The enamine-enamine tautomers of **S1** and **S2** and the aldehyde-aldehyde gossypol tautomer differ significantly in the electron density distribution within the naphthalene rings (Scheme 1) and therefore instead of the band of the ν(C═C) vibrations observed in the spectrum of gossypol at 1573 cm^{-1} the respective bands appear at 1524 and 1513 cm^{-1} in the spectrum of **S1** and at 1531 and 1518 cm^{-1} in the spectrum of **S2**. The additional medium intense band at 1647 cm^{-1} in the FT-IR spectrum of **S1** is assigned to the ν(C═C) vibrations of the allyl moieties. Thus, the spectroscopic and X-ray results consistently indicated the presence of the enamine-enamine tautomers of the Schiff bases **S1** and **S2** in the solid.

The FT-IR spectra of the Schiff bases **S1** and **S2** in solid and in solution in the range 1800–1500 cm^{-1} (Fig. 1S and 2S†) are comparable confirming the presence of the enamine-enamine tautomers for the two compounds in both states.

Stoichiometry of the protonation of gossypol Schiff bases determined by ESI measurements

The ESI mass spectra recorded for the **S1** and **S2** mixtures with $HClO_4$ acid (Table 1) indicate the exclusive formation of $[\mathbf{S1} + H]^+$ (*m/z* 597) and $[\mathbf{S2} + H]^+$ (*m/z* 771) monoprotonated species as well as $[\mathbf{S1} + 2H]^{2+}$ (*m/z* 299) and $[\mathbf{S2} + 2H]^{2+}$ (*m/z* 386) diprotonated ones, depending on the Schiff base : acid stoichiometry, respectively. The appearance of *m/z* signals at 258 and 194 in the respective ESI mass spectra of the 1 : 3 and 1 : 4 mixtures of **S2** with H^+ reveals the formation of $[\mathbf{S2} : 3H]^{3+}$ and $[\mathbf{S2} : 4H]^{4+}$ species, respectively. The fact that in the respective ESI mass spectra of various mixtures of Schiff bases with the acid only one *m/z* signal is detected (Table 1) indicates that in the gas phase no equilibrium between monoprotonated, diprotonated and unprotonated Schiff bases occurs. Thus, the equimolar addition of the proton to the Schiff bases leads to exclusive location of the proton at a specific site within the half of **S1** or **S2** molecule (Scheme 2a and b). The ESI data are taken into account in discussion of the potentiometric and semi-empirical results given below.

Acid–base properties of gossypol Schiff bases determined by potentiometric, FT-IR and ^{1}H NMR titration

Two different types of potentiometric titration curves of totally protonated **S1** and **S2** compounds were obtained with tetrabutylammonium hydroxide as a base in acetonitrile. An exemplary

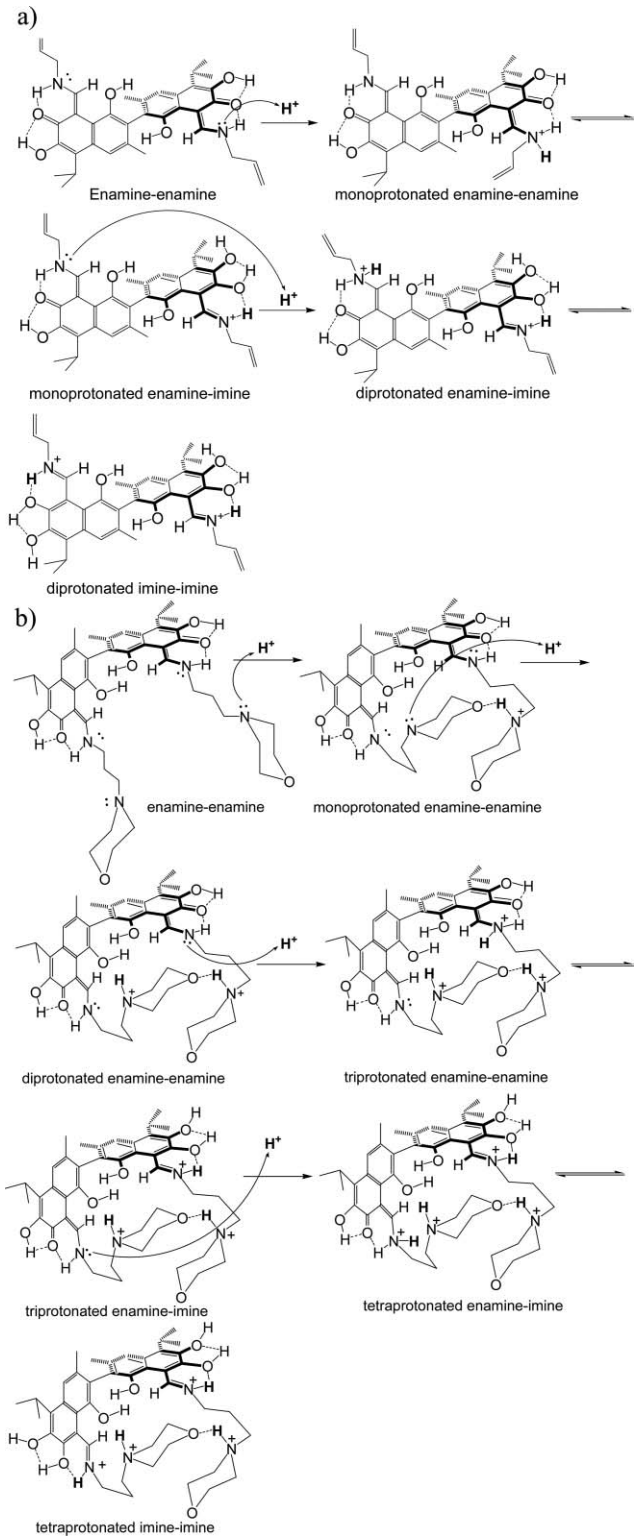

Scheme 2 The plausible mechanism of protonation of: a) **S1**, b) **S2** proposed on the basis of ESI MS, FT-IR, ^{1}H NMR, potentiometric and PM5 semi-empirical data.

curve recorded for **S2** is shown in Fig. 2. The experimental curves obtained for **S1** and **S2** show that deprotonation of the totally protonated Schiff bases proceeds *via* a minimum of two stages. The models taken into account in our potentiometric investigation

Table 2 The pK_a values of **S1** and **S2** Schiff bases determined using the potentiometric titration in acetonitrile solution

	pK_a value			
Schiff base	p$K_{a\,(1)}$	p$K_{a\,(2)}$	p$K_{a\,(3)}$	p$K_{a\,(4)}$
S1	10.87 ± 0.82	12.37 ± 0.89	—	—
S2	11.55 ± 0.65	12.51 ± 0.78	17.25 ± 1.25	22.65 ± 1.36

assume the presence of the following protonated species: model 1° – BH^+, model 2° – BH^+, BH_2^{2+}, model 3°– BH^+, BH_2^{2+}, BH_3^{3+}, model 4° – BH^+, BH_2^{2+}, BH_3^{3+}, BH_4^{4+}, where B is the Schiff base (**S1** or **S2**). The fit of the calculated potentiometric titration curves for models 1°–4° to the experimental ones obtained for **S1** and **S2** (Fig. 2) indicates the best correlation with the curves calculated for model 2° (**S1**) and for model 4° (**S2**) (Table 4S†). Thus, the pK_a values (Table 2) for **S1** Schiff base were calculated from the following equilibria:

$$BH_2^{2+} = BH^+ + H^+ \quad K_1 \tag{1}$$

$$BH^+ = B + H^+ \quad K_2 \tag{2}$$

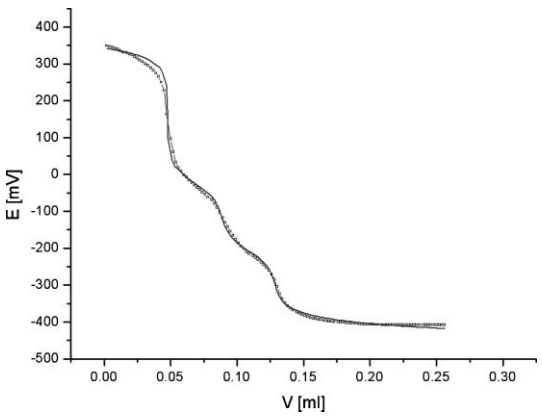

Fig. 2 The result of the fit of the theoretical curve (solid line) – model 4° – into the experimental one (squares) obtained from the potentiometric titration of totally protonated **S2** with the base.

For **S2** the pK_a values were determined for the equilibria given below:

$$BH_4^{4+} = BH_3^{3+} + H^+ \quad K_1 \tag{1}$$

$$BH_3^{3+} = BH_2^{2+} + H^+ \quad K_2 \tag{2}$$

$$BH_2^{2+} = BH^+ + H^+ \quad K_3 \tag{3}$$

$$BH^+ = B + H^+ \quad K_4 \tag{4}$$

The number of pK_a values determined for the Schiff bases by the potentiometric titration corresponds to the number of signals of protonated **S1** and **S2** species detected in the ESI MS spectra. As follows from Table 2 and ESI data discussed above (Table 1), **S1** contains two basic sites, while **S2** has four.

In order to determine the protonation sites within **S1** (Fig. 3S†) and **S2** (Fig. 3), the titrations with $HClO_4$ in acetonitrile monitored by FT-IR spectra were performed. Additionally, structural

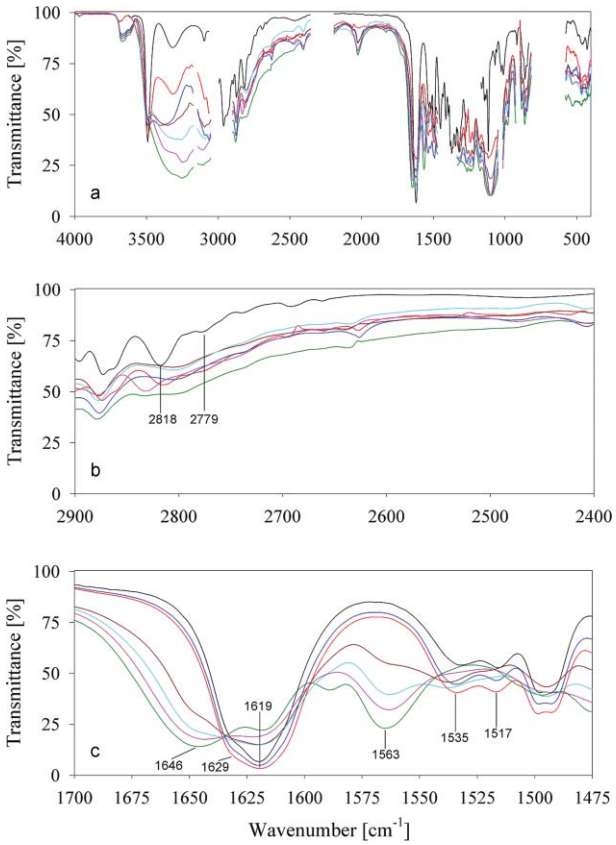

Fig. 3 Results of the titration of **S2** with $HClO_4$ controlled by the FT-IR spectra in the ranges: a) 4000–400 cm^{-1}, b) Bohlmann band region, c) 1700–1475 cm^{-1}; (black line) **S2**, (red line) **S2** : H^+, (dark blue line) **S2** : $2H^+$, (brown line) **S2** : $2.5H^+$, (light blue line) **S2** : $3H^+$, (violet line) **S2** : $3.5H^+$, (green line) **S2** : $4H^+$.

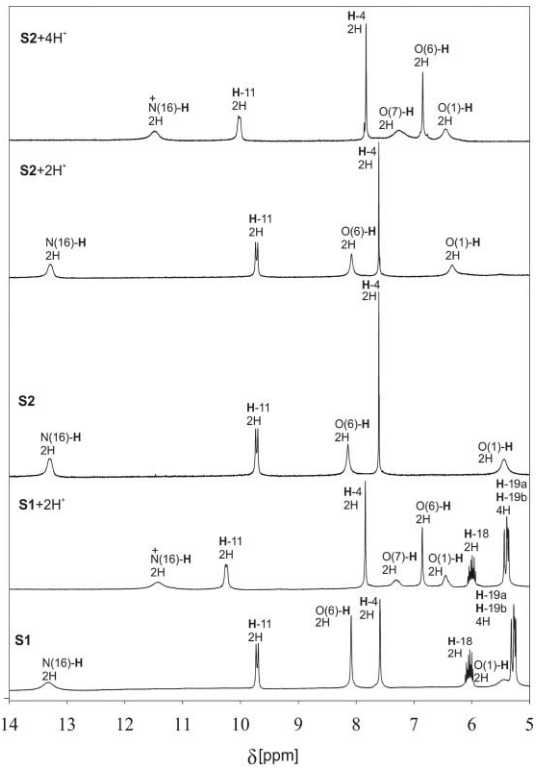

Fig. 4 ^1H NMR spectra of **S1** and **S2** as well as the mixtures: **S1** + $2HClO_4$, **S2** + $2HClO_4$, **S2** + $4HClO_4$ in CD_3CN.

changes after protonation of gossypol Schiff bases were investigated by ^1H NMR methods (Fig. 4). In FT-IR spectrum of **S1**-H^+ mixture (Fig. 3*S*), besides the characteristic bands at 1645, 1627, 1531 and 1518 cm^{-1} discussed above for the FT-IR spectra recorded in the solid, new ones arise at 1648 and 1565 cm^{-1}. The new band at 1565 cm^{-1} is assigned to the ν(C=C) naphthalene ring in the protonated imine-imine form of the Schiff base, whereas the other one at 1648 cm^{-1} is characteristic of δ(=$^+$N–H) vibrations. The presence of these bands and their absorptions provide the evidence that protonation results in the protonated imine form of one half of the **S1** molecule (Scheme 2a). This statement is consistent with the ESI data and with further FT-IR and ^1H NMR spectral changes observed after increasing the protonation stoichiometry, *i.e.* in the FT-IR spectrum of the **S1**–$2H^+$ (Fig 3S†) mixture the complete vanishing of the bands characteristic of the enamine-enamine tautomer (at 1627, 1531 and 1518 cm^{-1}) and increase in the band absorptions at 1565 cm^{-1}. The change of the enamine-enamine tautomeric form into protonated imine-imine one for **S1** after addition of the second proton is evidenced by ^1H NMR spectrum of the **S1**–$2H^+$ mixture in which a new signal assigned to the O(7)–H proton appeared in comparison to the **S1** spectrum (Fig. 4). The change of the tautomeric form within **S1** after the second protonation is manifested as a shift of the N(16)–H proton signal toward lower ppm values and a shift of the H-11 resonance toward higher ppm values (Fig. 4). The shielding of the N(16)–H proton signal can be explained by the formation of N^+(16)–H $\cdots$ O(7) intramolecular hydrogen bond within protonated imine-imine tautomer of **S1** weaker than N(16)–H $\cdots$ O(7) for the unprotonated **S1** molecule due to the appearance of the phenolic hydroxyl group C(7)–OH in the former instead of the carbonyl group C(7)=O in the latter. The deshielding of the H-11 proton signal, as well as the decrease in the $^3J_{H11-H16}$ coupling constant value from 13 Hz to 7 Hz in the **S1**–$2H^+$ spectrum relative to the spectrum of **S1**, reveal the presence of positive charge at the N^+(16) atoms after protonation.

Further addition of the acid to the **S1**–$2H^+$ mixture did not change the FT-IR spectrum in the analytical region 1700–1500 cm^{-1}, crucial for distinction of the tautomeric forms of gossypol derivatives. This result is in agreement with the pK_a values determined for **S1** (Table 2). The shift of the ν(C=C) band assigned to the allyl moieties from 1645 cm^{-1} to 1635 cm^{-1} in the spectra of **S1**–H^+ and **S1**–$2H^+$ results from lower π-electron density in these moieties due to their involvement in stabilisation of protonated imine-imine forms, as calculated by the PM5 method (Fig. 4Sa and b†). The $\Delta H_f°$ values of the most favourable structures of **S1**–H^+ and **S1**–$2H^+$ are given in Table 5S,† which lists also $\Delta H_f°$ values for other considered structures.

In the FT-IR spectra of 1 : 1 and 1 : 2 mixtures of **S2** with $HClO_4$ no changes in the band positions and their absorptions in the region 1700–1500 cm^{-1} are observed, when compared with the spectrum of the unprotonated form of **S2** (Fig. 3c). Furthermore, comparison of the ^1H NMR spectra of **S2** with that of **S2**–$2H^+$ (Fig. 4) indicates no changes in the position and multiplicity of the N(16)–H and H-11 proton signals and the absence of the O(7)–H proton signal after the protonation. The FT-IR and NMR results

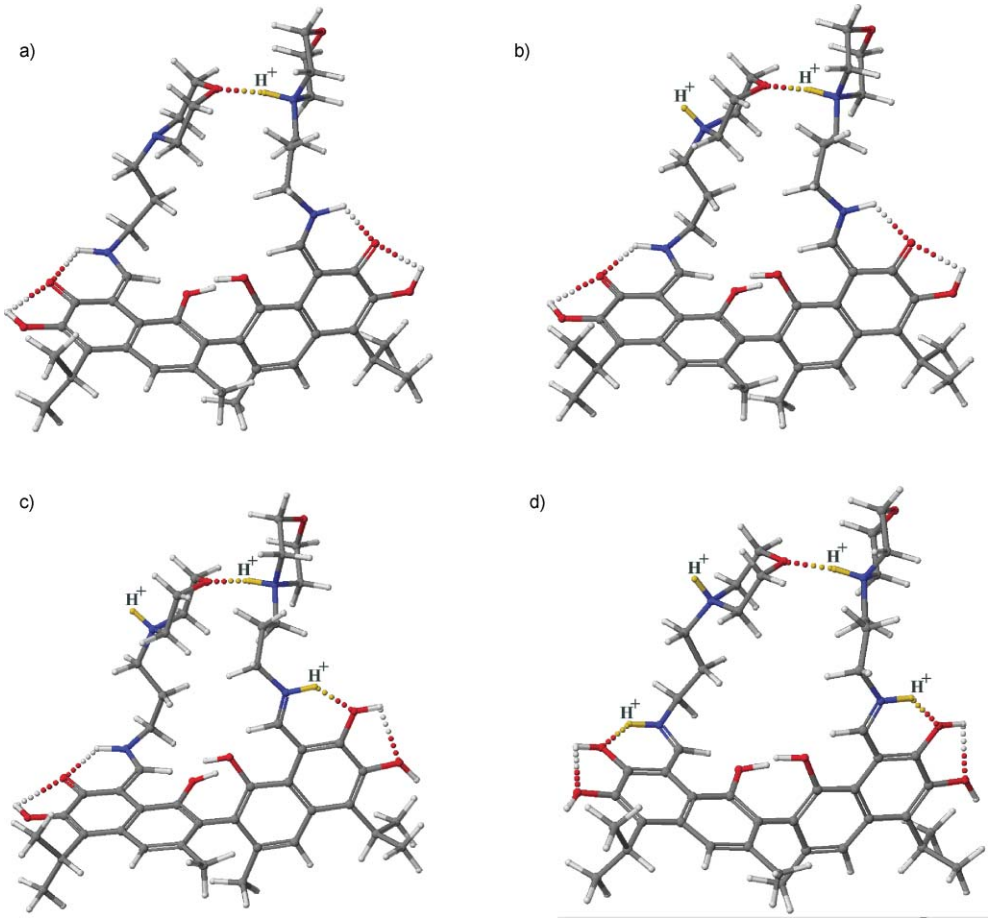

Fig. 5 The most favourable structures of the protonated **S2** Schiff base: a) **S2** : H^+, b) **S2** : $2H^+$, c) **S2** : $3H^+$, d) **S2** : $4H^+$, calculated by the PM5 method at semi-empirical level of theory; the excess protons are marked in yellow.

taken together clearly demonstrate that the excess protons are not localised at the Schiff base nitrogen atoms (N16) and therefore no change in the enamine-enamine tautomeric form of **S2** occurs up to **S2**–$2H^+$ stoichiometry (Scheme 2b). The question is about the protonation sites within the mono- and di-protonated **S2** molecules. The answer to this question is easier when comparing the FT-IR spectra of **S2**, **S2**–H^+ and **S2**–$2H^+$ in the Bohlmann band region 2700–2900 cm^{-1} (Fig. 3b). The Bohlmann bands are characteristic of N-bases possessing a lone electron pair not involved in the resonance phenomenon and alkyl groups at the N atom. The presence of these bands is related to the C–H stretching vibrations of the C–H bonds in the *trans*-arrangement to the lone electron pair at the N atom.[38–41] The Bohlmann bands of the propyl-morpholine moieties in the spectrum of **S2** are found at 2818 cm^{-1} and 2779 cm^{-1} (Fig. 3b). In the spectrum of **S2**–H^+ these bands are also present and their absorptions are lower, whereas in the spectrum of **S2**–$2H^+$ they vanish completely. This result indicates stepwise protonation of morpholine N-atoms in such a way that the first proton is localised at one of the two morpholine N-atoms, whereas the second proton is at the N-atom of the second morpholine moiety (Scheme 2b). This conclusion is in line with the most energetically favourable first and the second protonation sites within **S2** determined by the PM5 calculations (Fig. 5a and b). The $\Delta H_f°$ values of the protonated species as well as the protonation sites considered within **S1** and **S2**, for the PM5 semi-empirical calculations, are collected in Table 5S.†

The difference of several orders of magnitude between $pK_{a(4)}$ and $pK_{a(3)}$ values (Table 2), the highest energetic profit obtained for the calculated $\mathbf{S2}_{en\text{-}en}$–$H^+$(E) structure (the most negative value of $\Delta H_f°$—Table 5S,† structure shown in Fig. 5a) and the stepwise vanishing of the Bohlmann bands in the FT-IR spectra of protonated **S2** (Fig. 3b) suggest the formation of the heteroconjugated intramolecular N^+–H···O hydrogen bond between morpholine moieties [N···O distance = 2.84 Å, NHO angle = 171°] for the monoprotonated structure of **S2** (Scheme 2b). The dihedral angle (ω) between naphthalene planes, found in the crystal structure of unprotonated **S2**, is equal to 89° (see Supplementary Data†). The formation of the intramolecular hydrogen bond N^+–H···O between morpholine moieties changes the mutual orientation of the propyl-morpholine substituents and decreases the dihedral angle (ω) to *ca.* 70° (Fig. 5S†).

After addition of the acid to the **S2** above **S2**–$2H^+$ stoichiometry, the bands at 1563 cm^{-1} and 1646 cm^{-1} (Fig. 3c), characteristic of protonated imine-imine tautomeric form, arise at similar frequencies as in the spectra of **S1**–H^+ and **S1**–$2H^+$ mixtures (Fig 3S†). The stepwise increase in the band absorption at 1563 cm^{-1} and 1646 cm^{-1} with a simultaneous decrease in the band absorption at 1629 cm^{-1} from **S2**–$2H^+$ to **S2**–$4H^+$ stoichiometry (Fig. 3c) is clear evidence of the stepwise change of the enamine-enamine

into the protonated imine-imine tautomeric form. The tautomeric form change for **S2** is also well visible in the ^{1}H NMR spectrum of the **S2**–4H$^+$ mixture (Fig. 4) which is comparable in the 5–14 ppm range to that of **S1**–2H$^+$, discussed above.

As shown in Fig. 5b the second proton is localised at the nitrogen atom of the **S2** morpholine group and is not involved in intramolecular hydrogen-bonding, therefore the p$K_{a(3)}$ value is significantly lower than p$K_{a(4)}$ and comparable with pK_a ~17 determined in acetonitrile for morpholine and its N-alkyl derivatives.[42] In turn the p$K_{a(1)}$ and p$K_{a(2)}$ values of **S2**, resulting from the deprotonation of the Schiff base moieties, are virtually similar to those of **S1** (Table 2), and in these cases are independent of the amine substituent character, confirming that in **S1** only the Schiff base moieties are stepwise protonated (Fig. 4S†).

Conclusions

In summary, it has been shown that the enamine-enamine tautomeric form of gossypol Schiff bases changes stepwise into the protonated imine-imine form upon addition of various amounts of acid as indicated by potentiometric, FT-IR and ^{1}H NMR titration. Introduction of the propyl-morpholine moieties to the gossypol framework results in obtaining an efficient base with pK_a value higher than that of the proton sponge and within the pK_a range of such strong organic bases as DBU, TMG or phosphazenes and their derivatives.[43,44] We have shown that protonation of gossypol Schiff bases increases the number of phenolic groups in the molecule, which is important information for determination of the toxicology mechanism of action of gossypol aza-derivatives.

Experimental

Materials and methods

Gossypol was extracted from cotton seeds of *Gossypium herbaceum* following the procedure given in Ref. 19 The 3-morpholinopropylamine used was a commercial product of Aldrich. Gossypol Schiff base with 3-morpholinopropylamine (**S2**) was obtained by the procedure given in Ref. 21. Gossypol Schiff base with allylamine (**S1**) was synthesised by the procedure given in Ref. 25.

X-Ray structure determination of S2

A single crystal suitable for diffraction studies was grown as a very tiny plate, with dimensions of $0.35 \times 0.1 \times 0.01$ mm, therefore the data were collected at 105 K and the crystal was mounted in a mesh-loop with a small amount of perfluoropolyether. The X-ray diffraction measurements were carried out with a Super-Nova single-crystal diffractometer using hi-flux micro-focus Nova Cu-Kα radiation (λ = 1.54184 Å). Data collection and reduction were performed with CrysAlisPro software.[45] The structure was solved by direct methods with the SHELXS-97 program[46] and refined by full-matrix least-squares method on F^2 with SHELXL-97.[46] All non-hydrogen atoms were refined with anisotropic displacement parameters. The hydrogen atom positions were found in difference Fourier maps, however, for further refinement they were determined geometrically (C–H 0.93, C–H$_2$ 0.97, C–H$_3$ 0.96, N–H 0.86, O–H 0.82 Å) and their displacement parameters were set equal to 1.2U$_{eq}$(C,N,O). One of the morpholine fragments from the propyl-morpholine group attached to the amine N atom of the Schiff base was disordered over two positions. The crystal data and some details of data collection and structure refinement are given in Table 1S.† CCDC 763715 contains the supplementary crystallographic data for this paper.

ESI MS measurements

The ESI (Electrospray Ionisation) mass spectra were recorded on a Waters/Micromass (Manchester, UK) ZQ mass spectrometer equipped with a Harvard Apparatus syringe pump. The measurements were performed for samples being solutions of gossypol Schiff bases (**S1** or **S2**) (1×10^{-5} mol L^{-1}) with HClO$_4$ or HCl (1×10^{-5}, 2×10^{-5}, 3×10^{-5}, 4×10^{-5} mol L^{-1}) in acetonitrile. The ESI source potentials were: capillary 3 kV, lens 0.5 kV, extractor 4 V. For the standard ESI mass spectra the cone voltage was 10 V. The source temperature was 120 °C and the desolvation temperature was 300 °C. Nitrogen was used as the nebulising and desolvation gas at flow-rates of 100 and 300 L h^{-1}, respectively. Mass spectra were acquired in the positive ion detection mode with unit mass resolution at step size of 1 m/z unit. The mass range for ESI experiments was from m/z = 100 to m/z = 2500.

Potentiometric titration of S1 and S2

Potentiometric titrations were performed with the following equipment: an automatic titrator production Cerko Lab System with Hamilton's syringe (1 mL) interfaced with an IBM computer which the titrations were performed automatically by means of a suitable program Cerko Lab System ver. 3.OS-Expert. Constant-speed magnetic stirring was applied throughout. The temperature of the titration cell was kept at 25 °C by means of a Lauda E100 circulation thermostat. The pH combined electrode was bought from the Schott and it was calibrated on tetrabutylammonium 2,6-dinitrophenolate.[47,48] The solutions of the compounds studied and tetrabutylammonium hydroxide base were prepared directly before measurements. Aliquots (1.0 mL) of **S1**, **S2** solution, containing suitable amounts of HCl in acetonitrile, were potentiometrically titrated with standard tetrabutylammonium hydroxide in methanol ranged from 400 to –400 mV. The sample solution concentration ranged from 1×10^{-3} mol × dm^{-3} to 2×10^{-3} mol dm^{-3}, and the acid-to-solution ratios employed ranged to 4 : 1. The equilibrium constants of the complexes were determined using the software STOICHIO,[49] by minimisation of the differences between the theoretical model and the experimental data, following the method of Gauss–Newton–Marquart for nonlinear equations.

FT-IR titration of S1 and S2

S1 and **S2** Schiff bases (0.026 mmol) were dissolved in CH$_3$CN and titrated with the respective amount of HClO$_4$ in EtOH (0.026 mmol–0.104 mmol). Before every measurement of the FT-IR spectrum of the protonated Schiff base solution (0.5 mL of total volume) the mixture of EtOH–CH$_3$CN solvents was evaporated and subsequently five times 2 mL of acetonitrile (dried) were added to the sample and then evaporated to dryness. Finally, to the glassy residue of the protonated **S1** and **S2**, a portion of 0.5 mL of CH$_3$CN was added before FT-IR measurement.

The FT-IR spectra of **S1** and **S2** and their non-protonated and protonated species were recorded in the KBr pellets (1.5 mg per

200 mg) and in the acetonitrile solution (0.05 mol dm^{-3}). The FT-IR spectra were taken with an IFS 113v FT-IR spectrophotometer (Bruker, Karlsruhe) equipped with a DTGS detector; resolution 2 cm^{-1}, NSS = 125, range 4000–400 cm^{-1}. The Happ–Genzel apodisation function was used. All manipulations with the substances were performed in a carefully dried and CO_2-free glove box.

^{1}H NMR titration of S1 and S2

S1 and **S2** Schiff bases (0.026 mmol) were dissolved in CH_3CN and titrated with the respective amount of $HClO_4$ in EtOH (0.052 mmol and 0.104 mmol). Similarly as for FT-IR measurements, the mixture of CH_3CN–EtOH solvents was evaporated and subsequently five times 2 mL of acetonitrile (dried) were added to the sample and then evaporated to dryness. Finally, to the glassy residue of the protonated **S1** and **S2**, a portion of 0.8 mL of CD_3CN was added before every ^{1}H NMR measurement.

The ^{1}H NMR spectra of **S1**, **S2**, **S1** + 2$HClO_4$, **S2** + 2$HClO_4$, **S2** + 4$HClO_4$ were recorded in CD_3CN solutions using a Varian Gemini 300 MHz spectrometer. All spectra were locked to deuterium resonance of CD_3CN.

The ^{1}H NMR measurements in CD_3CN were carried out at the operating frequency 300.075 MHz; flip angle, pw = 8.8; spectral width, sw = 6500 Hz; acquisition time at = 4.0 s; relaxation delay, d_1 = 0.5 s; T = 293.0 K and using TMS as the internal standard. No window function or zero filling was used. Digital resolution was 0.2 Hz per point. The error of chemical shift value was 0.01 ppm.

PM5 semi-empirical calculations

PM5 calculations were performed using the Win Mopac 2007 program at the semiempirical level (Cache Work System Pro Version 7.5.085 – Fujitsu).[24,50,51] PM5 quantum semiempirical method uses the Schrödinger equation to determine the enthalpy of formation (H_f°) values of the protonated (H^+–$4H^+$) and unprotonated systems containing **S1** or **S2** molecules, bond strengths, atomic hybridisations, partial charges of the atoms and orbitals from the positions of the atoms and the net charge.

The protonation sites, tautomeric forms as well as hydrogen bond pattern stabilising tautomers were assumed taking into account the FT-IR and potentiometric data. The conformation of the two isopropyl groups were assumed from the crystal structures of **S2** (Fig. 1) and **S1**.[25] The structures of the complexes were initially optimised using the molecular mechanics (MM) – extensive global minimum energy conformation search with the Conflex/MM3 (WinMopac 2007). Global optimisation runs were carried out for all the complexes with H^+ using 1780–2326 local minimisations in each global optimisation. The lowest energetically structures of **S2**–H^+ containing protonated morpholine moiety, stabilised by the formation of N^+–H···O heteroconjugated intramolecular hydrogen bond, were obtained after the initial optimisation of the dihedral angle between the least-square planes [angle range 89°–70°] of the naphthalene moieties and subsequent conformational optimisation of propylene-morpholine fragments. The calculated energetically most favourable structures of conformers corresponding to the global minimum points were further optimised by the PM5 quantum method with the energy gradient not exceeding 5 kcal mol^{-1} in one step. In all cases full geometry optimisation of **S1** and **S2** and their protonated species' ($1H^+$–$4H^+$) structures was carried out without any symmetry constraints.

Supporting data

Elemental analysis data of **S1** and **S2** as well as their protonated species. The details of PM5 calculations. The FT-IR spectra of **S1** and **S2** in the solid (Fig. 1S), comparison of the FT-IR spectra **S1** and **S2** in acetonitrile (Fig. 2S), FT-IR spectra of protonated **S1** (Fig. 3S). Results of the fit of different equilibrium models for compounds **S1** and **S2** to potentiometric data (Table 4S). The lowest energy structures of the protonated **S1** (Fig. 4S). Comparison of the dihedral angle (ω) found in the structure of unprotonated **S2** (X-ray) with the dihedral angle calculated for monoprotonated **S2** (PM5) [Fig. 5S]. X-ray experimental details together with the results (Fig. 6S, Tables 1S–3S) and the detailed discussion of the structure of unprotonated **S2**. ΔH_f° values of the structures of **S1** and **S2** protonated molecules with the excess protons localised at the different sites considered (Table 5S).

Acknowledgements

Financial assistance from the Polish Ministry of Science and Higher Education–Grant No. N204 056 32/1432 is gratefully acknowledged by P. Przybylski.

References

1 R. D. Stipanovic, L. S. Puckhaber, J. Liu and A. A. Bell, *J. Agric. Food Chem.*, 2009, **57**, 566–571.
2 A. S. Bourinbaiar and S. Lee-Huang, *Contraception*, 1994, **49**, 131–137.
3 N. I. Baram, A. I. Ismailov, K. L. Ziyaev and K. Z. Rezhepov, *Chem. Nat. Compd.*, 2004, **40**, 199–205.
4 K. Sprogøe, D. Stærk, H. L. Ziegler, T. H. Jensen, S. B. Holm-Møller and J. W. Jaroszewski, *J. Nat. Prod.*, 2008, **71**, 516–519.
5 J. Jiang, W. Ye and Y. C. Lin, *Int. J. Mol. Med.*, 2009, **24**, 69–75.
6 Y.-W. Huang, L.-S. Wang, M. K. Dowd, P. J. Wan and Y. C. Lin, *Anticancer Res.*, 2009, **29**, 2179–2188.
7 R. Aneja, S. K. Dass, S. Prakash and R. Chandra, *Artif. Cell Blood Sub.*, 2004, **32**, 159–172.
8 P. Kovaci, *Curr. Med. Chem.*, 2003, **10**, 2711–2718.
9 K.-J. Lee, J. Rinchard, K. Dabrowski, I. Babiak, J. S. Ottobre and J. E. Christensen, *Anim. Feed Sci. Tech.*, 2006, **126**, 93–106.
10 M. Villaseñor, A. C. Coscioni, K. N. Galvão, R. C. Chebel and J. E. P. Santos, *J. Dairy Sci.*, 2008, **91**, 3015–3024.
11 V.-T. Dao, C. Gaspard, M. Mayer, G. H. Werner, S. N. Nguyen and R. J. Michelot, *Eur. J. Med. Chem.*, 2000, **35**, 805–813.
12 L. Zhang, H. Jiang, X. Cao, H. Zhao, F. Wang, Y. Cui and B. Jiang, *Eur. J. Med. Chem.*, 2009, **44**, 3961–3972.
13 J. A. Kenar, *J. Am. Oil Chem. Soc.*, 2006, **83**, 269–302.
14 P. Przybylski, A. Huczyński, K. Pyta, B. Brzezinski and F. Bartl, *Curr. Org. Chem.*, 2009, **13**, 124–148.
15 I. I. Tukfatullina, K. Z. Tilyabaev, A. Mamadrakhimov, B. A. Salakhutdinov, F. G. Kamaev, A. M. Yuldashev, M. K. Dowd, S. A. Talipov, B. T. Ibragimov and T. F. Aripov, *Chem. Nat. Compd.*, 2008, **44**, 440–445.
16 R. Adams, T. A. Geissman and J. D. Edwards, *Chem. Rev.*, 1960, **60**, 555–574.
17 M. K. Dowd and E. D. Stevens, *J. Chem. Crystallogr.*, 2007, **37**, 765–770.
18 N. I. Baram, Kh. L. Ziyaev, A. I. Ismailov, D. Ziyamov and Yu. S. Mangutova, *Chem. Nat. Compd.*, 2000, **36**, 185–188.
19 P. Przybylski, K. Pyta, D. Remlein-Starosta, G. Schroeder, B. Brzezinski and F. Bartl, *Bioorg. Med. Chem. Lett.*, 2009, **19**, 1996–2000.
20 P. Przybylski, K. Pyta, J. Stefańska, M. Ratajczak-Sitarz, A. Katrusiak, A. Huczyński and B. Brzezinski, *Eur. J. Med. Chem.*, 2009, **44**, 4393–4403.

21 P. Przybylski, J. Kira, G. Schroeder, B. Brzezinski and F. Bartl, *J. Phys. Chem. A*, 2008, **112**, 8061–8069 .
22 K. Z. Tilyabaev, S. A. Talipov, B. T. Ibragimov, M. K. Dowd and A. M. Yuldashev, *J. Chem. Crystallogr.*, 2009, **39**, 677–682.
23 P. Przybylski, K. Pyta, M. Ratajczak-Sitarz, A. Katrusiak and B. Brzezinski, *Pol. J. Chem.*, 2009, **83**, 747–759.
24 P. Przybylski, K. Pyta, B. Wicher, M. Gdaniec and B. Brzezinski, *J. Mol. Struct.*, 2008, **889**, 332–343.
25 P. Przybylski, K. Pyta, M. Ratajczak-Sitarz, A. Katrusiak and B. Brzezinski, *Struct. Chem.*, 2008, **19**, 983–995.
26 S. A. Talipov, B. T. Ibragimov, L. Yu. Izotova, Z. G. Tilyakov and D. N. Dalimov, *Khim. Prir. Soedin. (Russ.)*, 2004, 422–424.
27 S. A. Talipov, B. T. Ibragimov, K. M. Beketov, K. D. Praliev and T. F. Aripov, *Kristallografiya (Russ.)*, 2004, **49**, 841–846.
28 K. M. Beketov, S. A. Talipov, B. T. Ibragimov, K. D. Praliev and T. F. Aripov, *Kristallografiya (Russ.)*, 2003, **48**, 691–699.
29 P. Przybylski, M. Ratajczak-Sitarz, A. Katrusiak, W. Schilf, G. Wojciechowski and B. Brzezinski, *J. Mol. Struct.*, 2003, **655**, 293–300.
30 K. M. Beketov, B. T. Ibragimov, S. A. Talipov, K. Makhkamov and T. F. Aripov, *J. Inclusion Phenom. Mol. Recognit. Chem.*, 1997, **27**, 105–112.
31 M. Gdaniec, *J. Inclusion Phenom. Macrocyclic Chem.*, 1994, **17**, 365–376.
32 A. Filarowski, A. Koll and L. Sobczyk, *Curr. Org. Chem.*, 2009, **13**, 172–193.
33 A. Filarowski, A. Koll, M. Rospenk, I. Krol-Starzomska and P. E. Hansen, *J. Phys. Chem. A*, 2005, **109**, 4464–4473.
34 W. Schilf, B. Kamieński, B. Kołodziej, E. Grech, Z. Rozwadowski and T. Dziembowska, *J. Mol. Struct.*, 2002, **615**, 141–146.
35 T. M. Krygowski, K. Woźniak, R. Anulewicz, D. Pawlak, W. Kolodziejski, E. Grech and A. Szady, *J. Phys. Chem. A*, 1997, **101**, 9399–9404.
36 M. Gdaniec, B. T. Ibragimov and S. A. Talipov, *J. Inclusion Phenom. Mol. Recogn. Chem.*, 1990, **8**, 431–438.
37 M. K. Dowd, *Chirality*, 2003, **15**, 486–493.
38 S. Wolfe, H. B. Schlegel, M.-H. Whangbo and F. Bernardi, *Can. J. Chem.*, 1974, **52**, 3787–3792.
39 B. Brzezinski, H. Urjasz and G. Zundel, *J. Phys. Chem.*, 1996, **100**, 9021–9023.
40 A. K. Chandra, S. Parveen and T. Zeegers-Huyskens, *J. Phys. Chem. A*, 2007, **111**, 8884–8891.
41 S. Scheiner and T. Kar, *J. Phys. Chem. A*, 2008, **112**, 11854–11860.
42 M. Uudsemaa, T. Kanger, M. Lopp and T. Tamm, *Chem. Phys. Lett.*, 2010, **485**, 83–86.
43 I. Kaljurand, I. A. Koppel, A. Kutt, E.-I. Room, T. Rodima, I. Koppel, M. Mishima and I. Leito, *J. Phys. Chem. A*, 2007, **111**, 1245–1250.
44 I. Kaljurand, A. Kutt, L. Soovali, T. Rodima, V. Maemets, I. Leito and I. A. Koppel, *J. Org. Chem.*, 2005, **70**, 1019–1028.
45 *Oxford Diffraction. CrysAlisPro*, Version. 1.171.33.36d Oxford Diffraction Ltd., Yarnton, Oxfordshire, England, 2009.
46 G. M. Sheldrick, *Acta Cryst.*, 2008, **A64**, 112–122.
47 R. Wróbel and L. Chmurzyński, *Anal. Chim. Acta*, 2000, **405**, 303–308.
48 L. Chmurzyński, A. Wawrzynów and Z. Pawlak, *Electrochim. Acta*, 1990, **35**, 665–671.
49 J. Kostrowicki and A. Liwo, *Talanta*, 1990, **37**, 645–650.
50 *Cache Work System Pro Version 7.5.085 UserGuide*, Fujitsu, Beaverton, Oregon, USA, 2007.
51 J. J. P. Stewart, *J. Comp. Chem.*, 1989, **10**, 209–220.

